On particulate emissions from moving trains in a tunnel environment

Yingying Cha[a,*], Ulf Olofsson[a], Mats Gustafsson[b], Christer Johansson[c,d]

[a] Department of Machine Design, KTH Royal Institute of Technology, Stockholm, Sweden
[b] VTI The Swedish National Road and Transport Research Institute, Linköping, Sweden
[c] Department of Environmental Science and Analytical Chemistry, Stockholm University, Stockholm, Sweden
[d] SLB analys, Environment and Health Administration, Stockholm, Sweden

ARTICLE INFO

Keywords:
Railway tunnel
Airborne particulates
Individual train
Particle number concentration
Particulate size distribution

ABSTRACT

Increasing attention is being paid to airborne particles in railway environments because of their potential to adversely affect health. In this study, we investigate the contribution of moving trains to both the concentration and size distribution of particles in tunnel environments. Real-time measurements were taken with high time-resolution instruments at a railway station platform in a tunnel in Stockholm in January 2013. The results show that individual trains stopping and starting at the platform substantially elevate the particulate concentrations with a mobility diameter greater than 100 nm. Two size modes of the particulate number concentrations were obtained. A mode of around 170 nm occurs when a train moves, while the other mode peaks at about 30 nm when there is no train in the station. By using principal component analysis (PCA), three contributing sources were identified on the basis of the classification of the sizes of the particles, namely railway-related mechanical wear, suspension due to the movement of trains and sparking of electric-powered components. It is concluded that the particulate matter released by individual moving trains is a key contributor to fine particles (100–500 nm) on the railway platform in a tunnel.

1. Introduction

Researchers have noted high concentrations of airborne particles on subway platforms, particularly in tunnels and underground stations in daily use (Braně, 2006; Cartenì et al., 2015; Cheng et al., 2008; Johansson and Johansson, 2003; Kang et al., 2008; Kim et al., 2012, 2008; Mugica-Álvarez et al., 2012; Querol et al., 2012; Salma et al., 2007; Seaton et al., 2005). The highest exposure to airborne particles takes place on platforms rather than inside trains (Minguillón et al., 2012). For instance, in Stockholm the particulate level on an underground subway platform was reported to be several times higher than the 24-h limit on ambient PM10 (particles smaller than 10 μm in aerodynamic diameter size) set by the EU (Johansson and Johansson, 2003). Some authors attribute these high particulate levels to ambient traffic-related particulate pollutants (Braně, 2006; Cheng et al., 2008). Others attribute them to deterioration of subway stations' internal facilities or to train-related mechanical wear (Johansson and Johansson, 2003; Kim et al., 2008). Mugica-Álvarez et al. (2012) argue for the joint influence of railway-related sources and the ambient air. It has also been suggested that the problem is more severe at old subway systems than at newly designed stations. To be more specific, the particulate levels on old platforms were reported to be two to three times higher than those measured on newly constructed platforms (Querol et al., 2012). When an old subway platform was updated with an advanced optimized ventilation system, the particulate

* Corresponding author.
  E-mail address: yingcha@kth.se (Y. Cha).

concentration was estimated to have dropped sevenfold (Querol et al., 2012). In addition, a new design of platform screen doors has also contributed to improving the air quality on underground subway platforms by isolating the platforms from the pollutants in tunnels (Kim et al., 2012; Querol et al., 2012).

There are also those who attribute the high particle concentrations to the suspension of particles due to the turbulence caused by passing trains. It has been shown that train movement results in an increase in particulate mass concentration of up to 40% above an average value (Cartenì et al., 2015). Similar correlations between the increases in particulate levels on platforms and the passage of trains have also been reported in Cusack et al. (2015), Johansson and Johansson (2003), Martins et al. (2015), Salma et al. (2007). However, Gustafsson et al. (2006) found that even after washing a tunnel there were still very high levels of particulates, even though there was no longer any noticeable contribution from material deposited on the bedrock.

As has been reported by previous studies (Cusack et al., 2015; Olofsson, 2011; Sundh et al., 2009), different contributing sources and different generation mechanisms contribute to different size distributions of railway aerosols. For example, mechanical wear of wheel, rail and brake materials has been reported to generate a large number of particles in micron and even nanometre sizes. The nanometre fractions correspond to high sliding velocities (Olofsson, 2011; Sundh et al., 2009).

As a result of the different contributing sources, the chemical composition of railway aerosols depend on particle size. However, similar size distributions of some trace elements indicate similar sources (Cusack et al., 2015). Therefore, in spite of the difficulty of determining the exact sources of railway aerosols, the identification of different size modes of airborne particles can be regarded as one approach to source identification. For example, measurement with instruments with three-minute resolution shows that the distribution of sub-micron particles does not vary significantly throughout the day but maintains a unimodal size distribution of around 130 nm in mobility diameter (Cusack et al., 2015). However, when the subway is inoperative during the night and no train moves, the concentration of coarser particles ($> 5\,\mu m$) decreases drastically (Colombi et al., 2013; Cusack et al., 2015). Increases in particulate levels have been reported to be associated with passing trains (Cusack et al., 2015; Gustafsson et al., 2012; Johansson and Johansson, 2003; Martins et al., 2015; Salma et al., 2007). Gustafsson et al. (2012) have shown that the increased mass concentration per train movement frequency can be quite different between a subterranean train and a ground-level train. The underground value was calculated to be about 5 times higher than the ground-level value. It is therefore of interest to investigate how each individual train contributes to the particulate concentrations, and in particular to the size distributions, in order to better understand the exact contributing sources.

With this in mind, a series of real-time measurements were carried out continuously over a 24-h period at Arlanda Central (C) Stockholm, which is the same station studied as one of the underground sites in Gustafsson et al. (2012). High time-resolution instruments were used to capture the moments when a train stopped and started and when no trains were operating in the tunnel. The goal was to identify the contribution of individual trains to the airborne PM concentrations on an underground platform and provide further understanding of the contribution of individual trains to railway/subway aerosols.

2. Methodology

2.1. Sampling sites

The stationary measurements were carried out over 24 h (from 20:00 PM, 31st January to 08:00 AM, 1st February 2013), at the Arlanda Central (Arlanda C) station as part of a measurement campaign supported by the Swedish Transport Administration. Arlanda C is a railway station completed in 1999 and located directly below Arlanda Airport in Stockholm, Sweden. The platform (Fig. 1) on which the test apparatus was mounted lies inside a wide tunnel with an approximate length of 5000 m. The test instruments were placed in the end of the platform in order to have less influence from passengers. The tunnel ceiling is about 7.5 m above the platform level. The platform is approximately 354 m in length and 11 m in width, and is 0.5–1 m above the track level. It separates the two rail tracks on which southbound and northbound trains operate every day. The traffic passing through this tunnel is a mix of five types of electric trains, namely, X2, X40, X60, X50–55, and RC locomotive-driven trains. They are all powered by electrical pantograph-catenary systems. The brake systems used by the X2, X40, X60, and X50-55 are disc brakes combined with electric braking. Normally disc brakes are the main braking system at speeds of 30 km/h and slower. Note that the RC locomotive train sets do not use electric braking but instead combine disc brakes and block brakes. The main brakes on the locomotives are disc brakes, but block brakes can also be used for drag braking, in which a small constant load is applied to clean and roughen the wheels during periods of low-
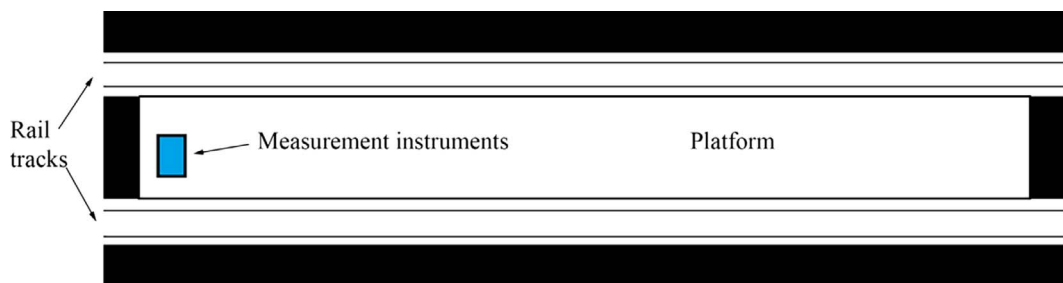

Fig. 1. A diagram of the Arlanda C platform showing the placement of the measurement instruments (a FMPS and an ELPI+).

adhesion or to control the train speed when going downhill. In the RC-driven train sets, the carriages used for passenger transport can have either disc or block brakes. Note that RC locomotives with different ages operate on this line, and that RC3 locomotives are an older generation than RC6 locomotives. Factors such as the weight of the train and the level of adhesion on the track may result in more manual operation of the RC trains than is the case with the more automated X2, X40, X60 and X50–55 trans. There were no mechanical ventilation and equalization shafts on the platform at Arlanda C station.

2.2. Sampling campaign and instruments

Particulate number concentrations and the size distributions of the aerosols on Arlanda C station platform were detected directly using a TSI Fast Mobility Particle Sizer Spectrometer (FMPS Model 3091) and an Electrical Low Pressure Impactor (ELPI+™). The former uses an electrical mobility technique with multiple, low-noise electrometers for particle detection and enables the measurement of particles ranging in size between 6.04 and 523.3 nm in electrical mobility equivalent diameter (D_p). The ELPI measures particles between 6 nm and 10 μm in aerodynamic diameter (D_a) through low pressure impactor and electrical detection with sensitive electrometers. D_a is defined as the diameter of a spherical particle of unit density (1 g/cm^3) having the same settling velocity as the actual particle, while D_p is defined as the diameter of a spherical particle having the same electrical mobility and the same bulk density as the irregular particle in question (Kumar et al., 2010).

The measurements in this study cover ultrafine (< 100 nm), fine (between 100 nm and 2.5 μm) and coarse fractions (between 2.5 and 10 μm). The measurement time resolution for both the FMPS and the ELPI+ was one second. The sampling flow rate was set to 10 L/min and the particle density 1 g/cm^3 for calculation of the mass concentration. The FMPS enables the monitored particulate matter to be counted by number concentrations with a total of 32 size-separated channels. The ELPI+ is composed of 15 stages and enables the measurement of airborne particles in 14 separate size classes. In addition, the use of impactor technology in the ELPI+ enables the collection of size-classified particles on aluminium substrates for further chemical and physical investigation. In order to prevent particle bounce and blow off, all filter substrates were coated with DS-515 grease spray before impactor measurements. The instruments were placed at one end of the platform (Fig. 1) with railings mounted to avoid interference by passengers. The sampling tests were conducted continuously in two periods: one between 9:30 and 18:30 on 31 January and the other one between 20:00 (31 January) and 08:00 am (1 February), 2013. However, the measurement data from the first period (9:30–18:30) could not be used due to instrumentation errors. The actual arrival and departure time for each train that either stopped at or passed through Arlanda C station was obtained from Stockholmståg and Trafikverket timetables.

2.3. Factor analysis

Principal component analysis (PCA) is a statistical tool used to extract the principal components from measured data to explain the majority of the variance (Jolliffe, 2002; Paatero et al., 2005). Before using this tool, the Kaiser-Meyer-Olkin (KMO) and Bartlett's tests were performed to determine whether the dataset in this study was suitable for such factor analysis. When these tests were positive, the data was analysed with the help of IBM SPSS Statistics 22 to determine the possible sources of the 14 different sizes of particles. A Varimax rotation was also applied to further distinguish the meaning of each extracted component.

The study of the different size fractions of particles detected by the ELPI+ (in 14 sized fractions) using factor analysis techniques enabled the identification of the main contributing sources. The relationship between each fraction of particles and the extracted principal components is reflected by their factor loadings (shown in the supplementary Table S-1). The higher the factor loading, the stronger the connection between that fraction and the source (Lawrence et al., 2013). In this study, a factor loading greater than 0.7 was considered as significant and the corresponding fraction was regarded as highly related to the source component, while those factors smaller than 0.7 were regarded as not significant. A loading smaller than 0.1 was disregarded in the analysis.

2.4. Chemical analysis

Particles collected on the size-separated filters by the ELPI+ were prepared for scanning electron microscopy (SEM) and energy dispersive spectrometer (EDs) analysis. All samples were gold sputter coated before analysis. The SEM observations were conducted using a conventional high-vacuum electron microscope. The accelerating voltage was set to be 15 keV. Other observation conditions such as beam current and magnification were selected based on the specific requirements for different sized samples.

3. Results

3.1. Particulate number and mass concentrations

Figs. 2 and 3 show the particulate number concentrations (PNC) and particulate mass concentrations (PMC) detected when trains are in operation and out of operation (between 00:50 and 04:50) at the Arlanda C station. These concentrations were averaged over 60 s from the original 1 Hz recorded data of the FMPS (Figs. 2(a) and 3(a)) and the ELPI+ (Figs. 2(b) and 3(b)). The variations in the PNC measured by the FMPS and the ELPI+ are similar (Fig. 2(a) and (b)). It can be seen that the PNC fluctuates significantly over the operational period, with a sharp peak around 21:30 followed by a substantial increase to a high level around 23:30. The increase around 23:30 would due to the movements of RC6 trains which only use mechanical braking (disc brakes). During the inoperative period when there is no traffic, the PNC level experiences a substantial increase, when there could be maintenance traffic operating
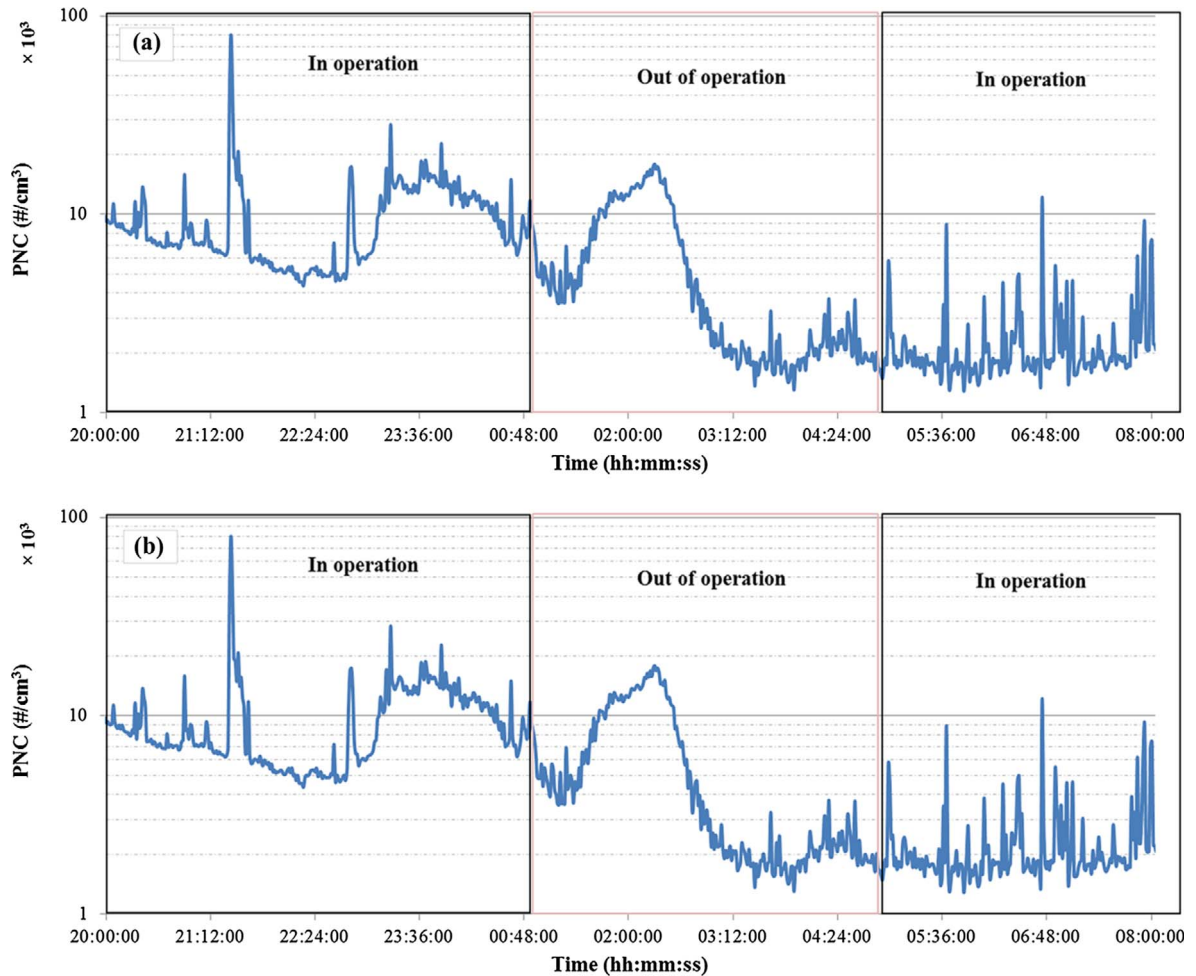
Fig. 2. The total particulate number concentration measured every 60 s between 20:00 and 08:00 (+ day), (a) by the FMPS (between 6.04 and 523.3 nm in mobility diameter size), and (b) by the ELPI+ (between 17 nm and 10 μm in aerodynamic diameter size).

with diesel exhaust emissions. Thereafter, it declines to a relatively stable but much lower level (with an average value of around 1500 #/cm^3 in Fig. 2(a) and 2000 #/cm^3 in Fig. 2(b)). It remains at a low level until the morning trains, which raise the PNC levels slightly, and then increases continuously with increasing operational traffic to fluctuate around a high level. Compared to the average value in the morning (1800 and 2300 #/cm^3 measured by the FMPS and the ELPI+, respectively), a much higher level is observed in the evening (5500 and 9700 #/cm^3 measured by the FMPS and the ELPI+, respectively).

The mass concentrations of the particles (within different size ranges) were obtained from the FMPS and ELPI+, as shown in Fig. 3(a) and (b), respectively. During the operational period in the evening (20:00–00:50), the average PM$_{10}$ (Fig. 3(b)) is around 140 μg/m^3, among which about 5.8 μg/m^3 is below 523.3 nm as measured by the FMPS. These values drop dramatically during the inoperative period to only 10 μg/m^3 for PM$_{10}$ (Fig. 3(b)) and 0.075 μg/m^3 of the fraction below 523.3 nm (Fig. 3(a)). In contrast to the PNC, instead of a substantial increase in the first half of the inoperative period, the mass concentrations decrease slightly. It could be interpreted that the increase of PNC during the inoperative period is mainly characterized by ultrafine and fine particles with small mass, which is hence not reflected in the mass concentration.

Fig. 4 shows size-separated PNCs measured by the FMPS (Fig. 4(a)) and the ELPI+ (Fig. 4(b) and (c)), with one second time resolution. The PNC value of fine particles (107.5–523.3 nm by FMPS and 0.108–0.64 μm by ELPI+) shows numerous sharp peaks when trains are in operation. These peaks mainly show up in the 100–300 nm range. In contrast, ultrafine particles tend to remain at more stable levels with a sharp increase only around 21:30 (in Fig. 4(b)) and substantial increases around 22:30 and 01:30 (in Fig. 4(a) and (b)). Analysis of the corresponding arrival and departure times of trains operating in the station indicates that some of the concentration peaks in fine fractions are connected to arriving trains (see supplementary file Figs. S-1 and S-2). These peaks decrease quickly to a low background level when a train leaves the station. No fine or coarse fractions are detected when the station is out of operation. However, we cannot attribute all the peaks in Fig. 4(a) and (c) to trains arriving at or leaving Arlanda C., for there is also express train traffic in a parallel tunnel connected to the tunnel studied.

Turning to particulate size distribution, Fig. 5 shows the size distribution of number concentration and Fig. 6 shows the size
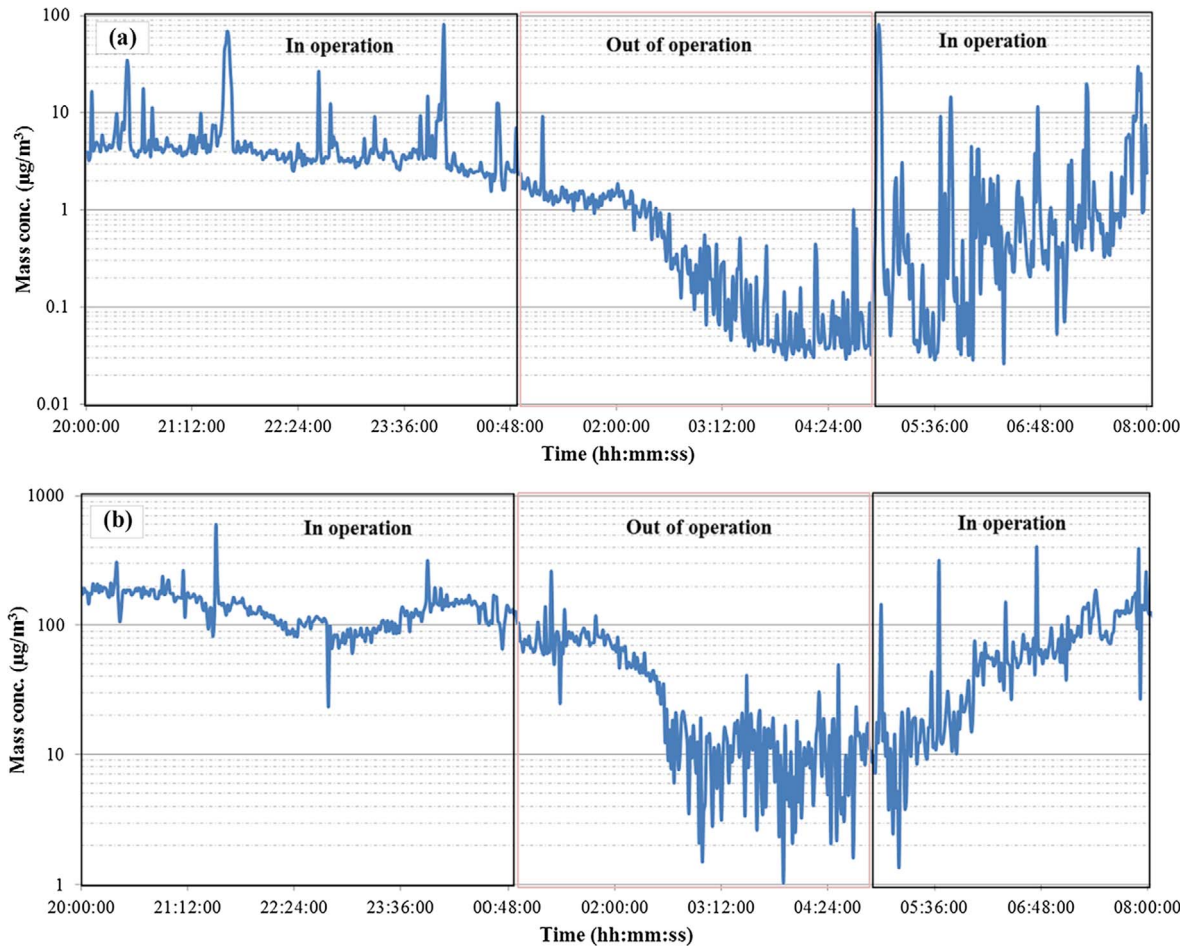
Fig. 3. Particulate mass concentration measured every 60 s by (a) the FMPS (between 6.04 and 523.3 nm in mobility diameter size), and (b) the ELPI+ (between 17 nm and 10 μm in aerodynamic diameter size).

distribution of mass concentration. The selected intervals capture three typical occasions: when a train stops and starts, a 10-min average with no traffic during the inoperative period, and the average over the whole test. Four types of trains (X40, X60, RC3 and RC6) were tracked. All the number and mass concentrations were averaged over 2 min when a train was present. It can be seen that quite low levels are detected in the absence of trains but that the levels are remarkably higher when trains were operating. Fig. 5 shows distinct differences in the number size distributions of particles collected during these intervals. To be more specific, the PNC has a dominant peak around 30 nm for both FMPS and ELPI+ results when there are no trains. Larger size particles (peak around 170-nm for both FMPS and ELPI+ measurement) increase when trains are moving in the station, except for an RC6 train that shows a substantial rise in ultrafine particles smaller than 30 nm. For all cases, particles smaller than 500 nm make up about 99% of the entire number concentration for both instruments.

When it comes to mass concentration, the size distributions vary significantly in nanometre size as shown in Fig. 6(a). When there is no train, the background mass concentration is dominated by large particles, while 250-nm particles dominate when trains are operating and in the averaged overall level measured by the FMPS. In terms of all the ultrafine, fine and coarse fractions measured by the ELPI+, dominant fractions are observed in coarser sizes both during inoperative and operational periods, as shown in Fig. 6(b). The movements of trains X40, X60, RC3 caused significant increases in coarse particles (> 6 μm) in mass concentration, unlike train RC6, for which the level of particles was similar to the overall average level. Additionally, small peaks are observed in the fine regime around 400 nm corresponding to the movements of trains X40, X60, RC3.

3.2. Particle element composition

Chemical analysis was carried out using a SEM (combined with EDS) to determine the elemental contents of particles in the two dominant size modes, 30 nm for the background environment without trains operating and 170 nm when trains are operating. For the 30-nm mode, the proportion of each element was calculated from the average of four scanned points. Some error can be expected for the specific mass proportion of single particles due to the detection limit of volume, which is 1 μm³. The elements present in the 170-
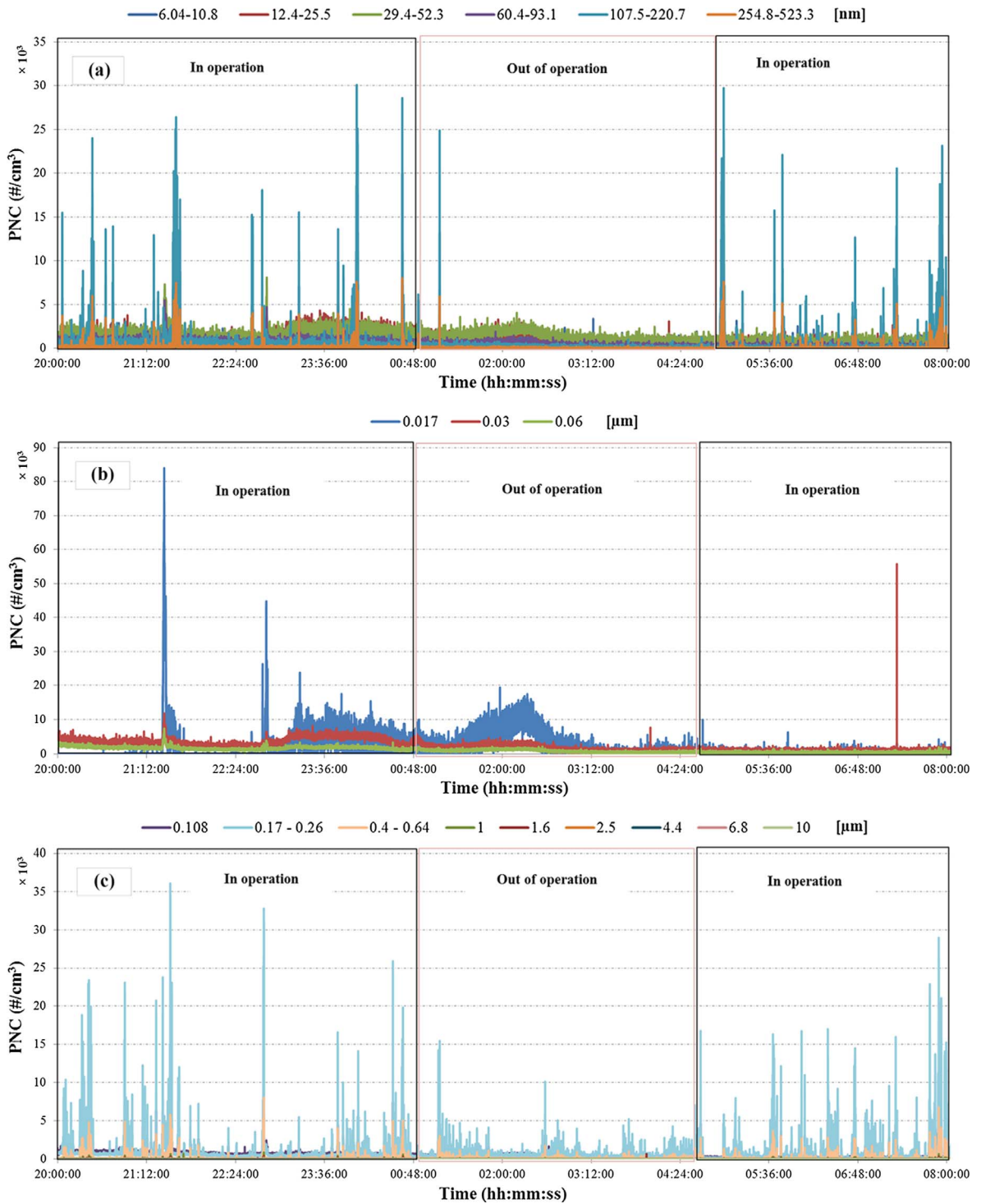
Fig. 4. Size-separated concentrations of the particles measured every 1 s (a) by the FMPS (between 6.04 and 523.3 nm in mobility diameter size), (b) by the ELPI+ (smaller than 60 nm in aerodynamic diameter size), and (c) by the ELPI+ (between 108 nm and 10 μm in aerodynamic diameter size).

nm mode were calculated by scanning two areas. Here the specific values are more reliable, since each area has a volume greater than 1 μm³. Although the exact numerical values should be approached with caution, the observations regarding the presence of specific elements are reliable. The elements contained in those two size fractions are shown in Table 1. The presence of copper and silver in the 30-nm fraction indicates a contribution from the pantograph-catenary system, which is the main electric power supply for trains in the Arlanda C tunnel. The chemical composition of copper alloy wires used for the catenary system in Arlanda is CuAg0.1 (Cu
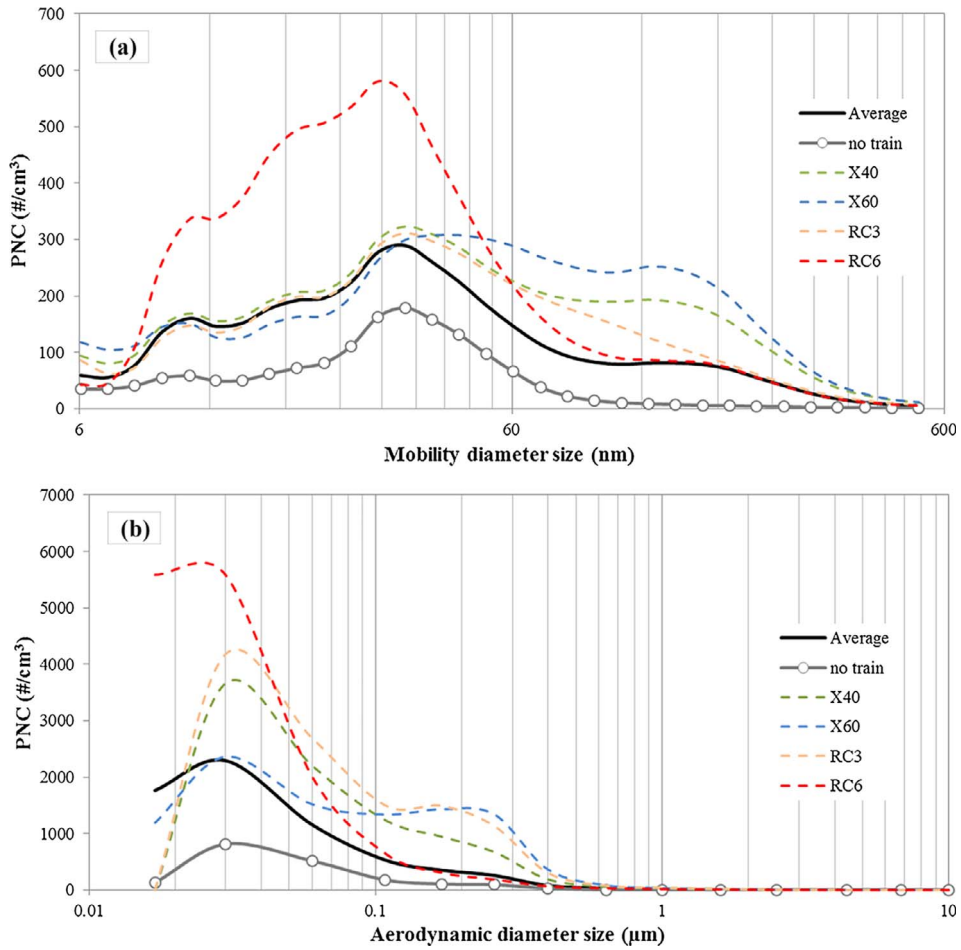
Fig. 5. Particulate size distribution of number concentration measured every 1 s by (a) the FMPS and (b) the ELPI+, capturing three occasions: average level over the total measurement time; average over 10 min (03:20–03:30) when no train operates; average over 2 min when different types of train are moving (20:20–20:22 is for X40 train, 22:25–22:47 for X60, 20:04–20:06 for RC3, and 23:35–23:37 for RC6).

99.8%, Bi 0.0005%, O 0.04%, and Ag 0.12%), and is the only source that could contribute Ag in the tunnel. Compared to the ultrafine fraction, the contents of the 170-nm sized particles are more complicated and include molybdenum (Mo), barium (Ba), and some crustal elements magnesium (Mg), silicon (Si), calcium (Ca).

3.3. Application of factor analysis

Since the ELPI+ measurement results cover a wide particle size range (between 6 nm and 10 μm), a principal component analysis (PCA) was carried out only for the ELPI+ data. Before performing the PCA, we used KMO and Bartlett's tests to determine the feasibility of using PCA for our data. The KMO measure yielded a value of 0.888 for the PNCs data measured by the ELPI+. Bartlett's test of both measurements rejected the hypothesis that the correlation matrix is an identity matrix, indicating that the dataset is suitable for factor analysis. Three principal components were extracted by PCA from the 14 sized fractions, as shown in Fig. 7. These extracted components contain at least 90% of the information of the original dataset.

Among the 14 sized fractions measured by the ELPI+, component one (C1) explains 59.58% of the total variance and has strong positive loadings with large particles (greater than 500 nm). The number concentration of particles greater than 500 nm (corresponding to C1) show no noticeable change when trains operate, but their mass concentration increases significantly when trains operate. Component two (C2) explains 16.28% of the total variance, is highly associated with particles with sizes between 100 and 500 nm. As illustrated above in Figs. 4 and 5, the levels of fine particles (100–500 nm) are strongly correlated with moving trains with respect to number concentration, and hence the particles comprising component two are assumed to be directly related to the movement of trains. Component three (C3) explains 13.67% of the total variance and is determined by ultrafine particles (smaller than 100 nm). The behaviour of ultrafine particles (corresponding to C3) is complicated, and will be further discussed in the next section.
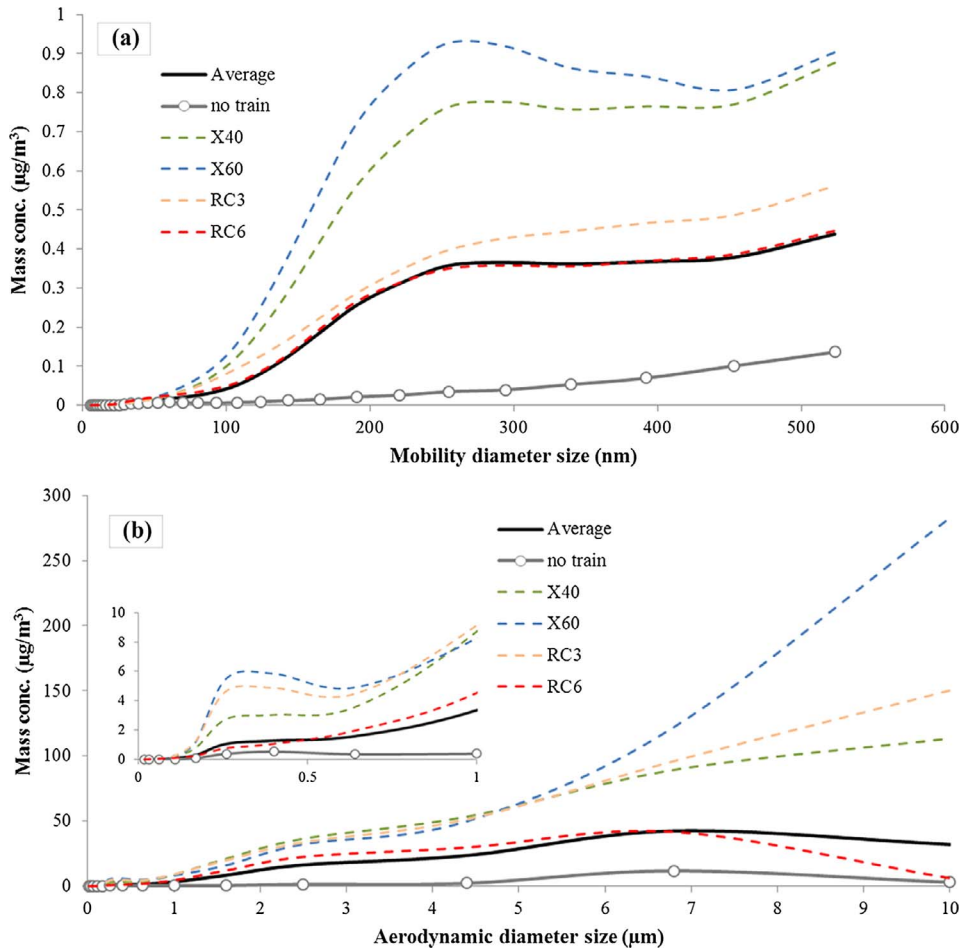
Fig. 6. Particulate size distribution of mass concentration measured every 1 s by (a) the FMPS and (b) the ELPI+, capturing three occasions: average level over the total measurement time; average over 10 min (03:20–03:30) when no train operates; average over 2 min when different types of train are moving (20:20–20:22 is for X40 train, 22:25–22:47 for X60, 20:04–20:06 for RC3, and 23:35–23:37 for RC6).

Table 1
Elemental contents of the particles of 30-nm and 170-nm size mode; oxygen and carbon were also observed but are not shown here.

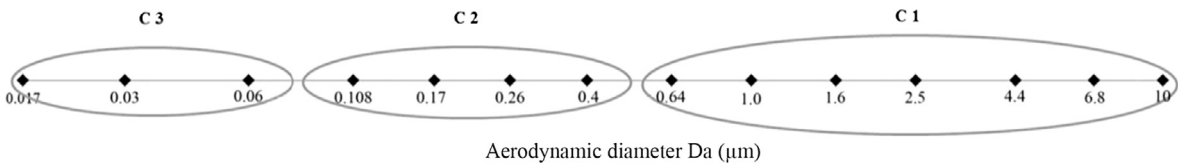| Fraction	Elemental contents										
30 nm	Fe	Cu	Zn	Ag	W						
170 nm	Fe	Cu	Zn	Ag	Mn	Ba	Mg	Mo	Si	Ca	P

Fig. 7. Principal components extracted from the ELPI+ measurement of size-separated particles: C1, C2, and C3.

4. Discussion

4.1. Particulate concentrations, size distributions, and chemical compositions

High time-resolution instruments were used to investigate the influence of individual trains on platform particulate matter. The results indicate that moving trains affect particulate concentrations and size distributions. When trains are operational both the

number and mass concentrations are relatively high (with average values of 140 μg/m^3 and 9.7 × 10^3 particles/cm^3 for PM$_{10}$ and PNC, respectively). This mass concentration level exceeds the limit PM10 value for outdoor air set by European commission (that is 50 μg/m^3 for averaging over 24 h) (European commision, n.d.), while no legislation on the limitation of particle number concentration released yet. However, both levels decrease to quite low values (10 μg/m^3 and 2.0 × 10^3 particles/cm^3, respectively) during the inoperative period. The increase in particulate number concentration starts when morning trains begin. The reduction begins after the departure of the last train. Thereafter the platform becomes clean apart from the increases in nanometre particle concentration around 22:30 and 01:30 during the inoperative period. These increases cannot be explained by train movement. The frequency of passing trains is regarded as a key cause of such increases in particles during the day (Johansson and Johansson, 2003; Salma et al., 2007). The maximum levels usually occur during the morning and afternoon rush hours when the train frequency is greatest (Cusack et al., 2015; Salma et al., 2007). However, in this case the increase in number and mass concentrations detected during the start of the morning rush hours in our study are not as high as might be expected. The different results may be due to different train frequencies, different particulate size fractions detected, different measurement methods or a different time resolution applied to determine the concentrations.

Substantial increases in the particulate number concentrations are observed to correspond to the movement of trains (Fig. 4). It is of interest that most train types give rise to fine particles, particularly in the 170-nm size mode, while one type of train gives rise to a nanometre fraction smaller than 30 nm, as shown in Fig. 5. Usually, increases in nanometre sizes can be attributed to causes such as different types of train operating in specific conditions (for example, at a high speed or with sparking of pantograph materials). Sundh et al. (2009) simulated friction wear between wheel and rail material and found that a given sliding velocity (0.4 m/s) generated a large amount of ultrafine particles smaller than 40 nm. It has also been suggested that hot processes such as smelting or sparking of metal materials in industrial plants generate ultrafine particles of about 30 nm diameter (Elihn and Berg, 2009). Disc brakes generate ultrafine airborne particles if the disc brake temperature is above the critical limit (Alemani et al., 2015). In our study, the train type that causes a rise in ultrafine particles is a locomotive-driven train RC6. In contrast to the other train types, the RC6 locomotives and their carriages use only mechanical brakes. The presence of silver and copper in the 30-nm mode (Table 1) indicates that the sparking of catenary wire also could be a noticeable contributor to ultrafine particles.

In general, the mechanical wear of brake, wheel and rail materials emits particles of aerodynamic diameter sizes ranging from ultrafine to coarse fractions, with a dominant peak at 350 nm in number concentration (Abbasi et al., 2011; Olofsson, 2011; Sundh et al., 2009). If the average density of these metal materials is estimated to be 4–5 g/cm^3 (Fridell et al., 2010; Salma et al., 2007; Sanders et al., 2003), then the number concentrations would peak at the mobility diameter size of 160–170 nm in these studies (Abbasi et al., 2011; Olofsson, 2011; Sundh et al., 2009). This provides an interesting agreement with the dominant peak (170-nm D$_p$) associated with train movement in our study. It suggests an alternative source for the 170-nm mode: the wear of metallic materials (for example wheel on rail and disc brakes) rather than from resuspended matter.

By washing the tunnel walls and the floor of the platform, (Gustafsson et al., 2006) showed that a dominant proportion of the particles at the Arlanda C station are not related to resuspension. Moreover, the presence of the elements Fe, Mn, Cu, Zn, Mo, Mg, Si, Ca, Ba and P in 170-nm sized particles further supports our speculation that suspension is not the major source. Those elements (Fe, Mg, Ca, Si, Ba, Mn, Zn, P, Cu and a small quantity of Mo) are characteristic components within the brake pads utilized in the X60 commuter trains. Their presence suggests that the source of the particles is likely to be mechanical wear mainly from brake pads. This finding contrasts with previous research that attributed the increase in particles only to suspension due to wind blasts caused by the trains (Martins et al., 2015) or to polluted air pushed from the tunnel as trains entered the station (Cusack et al., 2015; Salma et al., 2007). Instead, our result is similar to some other studies that conclude that brake and wheel-rail wear are the main source of PM in these environments (Cha et al., 2016; Moreno et al., 2015; Salma et al., 2007). We speculate that the contributing sources of platform particulate matter may vary at different stations.

4.2. Contributing sources of the size-separated particles

The extracted three components explain about 90% of the data, providing a feasible statistical method to relate the size-separated particles to different contributing sources. As clearly illustrated in Fig. 7, the detected particle fractions can be sorted into three groups on the basis of the extracted components, namely C1 (0.6–10 μm), C2 (100–500 nm), and C3 (10–80 nm). Their percentages in the total particle concentrations (mass concentration of 140 μg/m^3, number concentration of 9.7 × 103 #/cm^3) during train operational period are: C1 (98.06%, 1.05%), C2 (1.91%, 17.36%), and C3 (0.04%, 79.59%).

C2 consists of fine particles with a diameter greater than 100 nm and smaller than 500 nm. It is expected that these particles are directly produced by the operation of trains. This group of particles shows significant increases (170-nm mode being dominant) when individual trains enter the station and decreases rapidly to the stable background level after the trains departed. An even lower level of this fraction is detected during the inoperative period at night. As discussed in Section 4.1, experiments suggest that the 170-nm mode originates from metal released by the wear of brakes, wheels or rails. We therefore attribute C2 (100–500 nm) mainly to the mechanical wear of brake-wheel and wheel-rail contacts that occurs when a train moves in the station, although a certain amount of ultrafine particles smaller than 100 nm were also detected during a friction test of wheel-rail sliding contact (Sundh et al., 2009), which could attribute to specific conditions.

C1 consists of particles greater than 600 nm. This coarse fraction is more or less invisible when focusing on number concentration. However, it is dominant when considering mass concentration. It is closely correlated to the train traffic in mass concentration (Fig. 6). Suspension of dust induced by the moving trains would be the main contributor.

C3 is strongly associated with ultrafine particles smaller than 100 nm. It remains smooth and steady and changes little with the

movement of trains, except for one specific locomotive train RC6, indicating origins other than locally moving trains. The main sources of ultrafine particles (C3) could include particles generated by some special trains that are associated with sparking or unusual operating conditions such as using only mechanical block brakes. Another possible cause is vehicle exhaust emissions that are transported or diffused from the outdoors through air exchange or through the wind turbulence caused by moving trains (Cusack et al., 2015; Martins et al., 2015; Salma et al., 2007). However, this is not the case at Arlanda C station, since there is no ventilation system and it is not close to any roads with high vehicle traffic. Other research conducted in the same tunnel concluded that emissions of ultrafine particles are related to the movement of electric-powered trains and not to fuel combustion (Gustafsson et al., 2012).

5. Conclusion

The air on subway platforms has been reported to be more polluted than the ambient air (Cartenì et al., 2015; Kim et al., 2008). In the current work, a continuous 24-h test was carried out to study the contribution of individual moving trains to the particulate matter on an underground platform, particularly as regards concentrations and size distributions. Intensive real-time measurements were performed with high time-resolution instruments to capture the intervals when trains are in and out of operation.

The results show that the average particulate number and mass concentrations during the operational period are substantially higher (by factors of about 5 and 14, respectively) than those measured during the inoperative period. It is revealed that the particulate matter released by operational trains is a key component of particles in fine sizes (100–500 nm) with a peak around 170 nm. In addition, there is a significant difference in particulate size distribution when trains are in or out of operation. The former situation is dominated by fine particles with a size mode of 170 nm for most trains, while the latter is predominantly occupied by an ultrafine mode of 30 nm. An RC train contributes more ultrafine particles than other trains because it uses only mechanical brakes. Three different contributing sources corresponding to three groups of size-separated particles (between 6.04 nm and 10 μm) were identified by using principal component analysis. In these three groups, we conclude that the fine fraction (100–500 nm) is generated directly by railway-related mechanical wear and the coarse one (0.5–10 μm) is connected to movements of trains. The source of the remaining ultrafine group (< 100 nm) is not clear, but it is highly likely to be related to electric-powered trains with mechanical brakes.

Appendix A. Supplementary material

Supplementary data associated with this article can be found, in the online version, at http://dx.doi.org/10.1016/j.trd.2017.12.016.

References

Abbasi, S., Wahlström, J., Olander, L., Larsson, C., Olofsson, U., Sellgren, U., 2011. A study of airborne wear particles generated from organic railway brake pads and brake discs. Wear 273, 93–99. http://dx.doi.org/10.1016/j.wear.2011.04.013.
Alemani, M., Nosko, O., Metinoz, I., Olofsson, U., 2015. A study on emission of airborne wear particles from car brake friction pairs. SAE Int. J. Mater. Manuf. 9, 147–157.
Braniš, M., 2006. The contribution of ambient sources to particulate pollution in spaces and trains of the Prague underground transport system. Atmos. Environ. 40, 348–356. http://dx.doi.org/10.1016/j.atmosenv.2005.09.060.
Cartenì, A., Cascetta, F., Campana, S., 2015. Underground and ground-level particulate matter concentrations in an Italian metro system. Atmos. Environ. 101, 328–337. http://dx.doi.org/10.1016/j.atmosenv.2014.11.030.
Cha, Y., Abbasi, S., Olofsson, U., 2016. Indoor and outdoor measurement of airborne particulates on a commuter train running partly in tunnels. Proc. Inst. Mech. Eng. Part F J. Rail Rapid Transit 1–11. http://dx.doi.org/10.1177/0954409716642492.
Cheng, Y.-H., Lin, Y.-L., Liu, C.-C., 2008. Levels of PM10 and PM2.5 in Taipei rapid transit system. Atmos. Environ. 42, 7242–7249. http://dx.doi.org/10.1016/j.atmosenv.2008.07.011.
Colombi, C., Angius, S., Gianelle, V., Lazzarini, M., 2013. Particulate matter concentrations, physical characteristics and elemental composition in the Milan underground transport system. Atmos. Environ. 70, 166–178. http://dx.doi.org/10.1016/j.atmosenv.2013.01.035.
Cusack, M., Talbot, N., Ondráček, J., Minguillón, M.C., Martins, V., Klouda, K., Schwarz, J., Ždímal, V., 2015. Variability of aerosols and chemical composition of PM10, PM2.5 and PM1 on a platform of the Prague underground metro. Atmos. Environ. 118, 176–183. http://dx.doi.org/10.1016/j.atmosenv.2015.08.013.
Elihn, K., Berg, P., 2009. Ultrafine particle characteristics in seven industrial plants. Ann. Occup. Hyg. 53, 475–484. http://dx.doi.org/10.1093/annhyg/mep033.
European commision, n.d. Air Quality Standards [WWW Document]. URL http://ec.europa.eu/environment/air/quality/standards.htm (accessed 11.25.17).
Fridell, E., Ferm, M., Ekberg, A., 2010. Emissions of particulate matters from railways – emission factors and condition monitoring. Transp. Res. Part D Transp. Environ. 15, 240–245. http://dx.doi.org/10.1016/j.trd.2010.02.006.
Gustafsson, M., Blomqvist, G., Dahl, A., Gudmundsson, A., Swietlicki, E., 2006. Inandningsbara partiklar i järnvägsmiljöer.
Gustafsson, M., Blomqvist, G., Swietlicki, E., Dahl, A., Gudmundsson, A., 2012. Inhalable railroad particles at ground level and subterranean stations – physical and chemical properties and relation to train traffic. Transp. Res. Part D Transp. Environ. 17, 277–285. http://dx.doi.org/10.1016/j.trd.2011.12.006.
Johansson, C., Johansson, P.-Å., 2003. Particulate matter in the underground of Stockholm. Atmos. Environ. 37, 3–9.
Jolliffe, I.T., 2002. Principal Component Analysis, second ed. Encycl. Stat. Behav. Sci. vol. 30, pp. 487. http://doi.org/10.2307/1270093.
Kang, S., Hwang, H., Park, Y., Kim, H., Ro, C.-U., 2008. Chemical compositions of subway particles in seoul, korea determined by a quantitative single particle analysis. Environ. Sci. Technol. 42, 9051–9057. http://dx.doi.org/10.1021/es802267b.
Kim, K.H., Ho, D.X., Jeon, J.S., Kim, J.C., 2012. A noticeable shift in particulate matter levels after platform screen door installation in a Korean subway station. Atmos. Environ. 49, 219–223. http://dx.doi.org/10.1016/j.atmosenv.2011.11.058.
Kim, K.Y., Kim, Y.S., Roh, Y.M., Lee, C.M., Kim, C.N., 2008. Spatial distribution of particulate matter (PM10 and PM2.5) in Seoul Metropolitan Subway stations. J. Hazard. Mater. 154, 440–443. http://dx.doi.org/10.1016/j.jhazmat.2007.10.042.
Kumar, P., Robins, A., Vardoulakis, S., Britter, R., 2010. A review of the characteristics of nanoparticles in the urban atmosphere and the prospects for developing regulatory controls. Atmos. Environ. 44, 5035–5052. http://dx.doi.org/10.1016/j.atmosenv.2010.08.016.
Lawrence, S., Sokhi, R., Ravindra, K., Mao, H., Prain, H.D., Bull, I.D., 2013. Source apportionment of traffic emissions of particulate matter using tunnel measurements. Atmos. Environ. 77, 548–557. http://dx.doi.org/10.1016/j.atmosenv.2013.03.040.
Martins, V., Moreno, T., Minguillón, M.C., Amato, F., de Miguel, E., Capdevila, M., Querol, X., 2015. Exposure to airborne particulate matter in the subway system. Sci. Total Environ. 511, 711–722. http://dx.doi.org/10.1016/j.scitotenv.2014.12.013.

Minguillón, M.C., Schembari, A., Triguero-Mas, M., de Nazelle, A., Dadvand, P., Figueras, F., Salvado, J.A., Grimalt, J.O., Nieuwenhuijsen, M., Querol, X., 2012. Source apportionment of indoor, outdoor and personal PM2.5 exposure of pregnant women in Barcelona. Spain. Atmos. Environ. 59, 426–436. http://dx.doi.org/10.1016/j.atmosenv.2012.04.052.

Moreno, T., Martins, V., Querol, X., Jones, T., BéruBé, K., Minguillón, M.C., Amato, F., Capdevila, M., de Miguel, E., Centelles, S., Gibbons, W., 2015. A new look at inhalable metalliferous airborne particles on rail subway platforms. Sci. Total Environ. 505, 367–375. http://dx.doi.org/10.1016/j.scitotenv.2014.10.013.

Mugica-Álvarez, V., Figueroa-Lara, J., Romero-Romo, M., Sepúlvea-Sánchez, J., López-Moreno, T., 2012. Concentrations and properties of airborne particles in the Mexico City subway system. Atmos. Environ. 49, 284–293. http://dx.doi.org/10.1016/j.atmosenv.2011.11.038.

Olofsson, U., 2011. A study of airborne wear particles generated from the train traffic—block braking simulation in a pin-on-disc machine. Wear 271, 86–91. http://dx.doi.org/10.1016/j.wear.2010.10.016.

Paatero, P., Hopke, P.K., Begum, B.A., Biswas, S.K., 2005. A graphical diagnostic method for assessing the rotation in factor analytical models of atmospheric pollution. Atmos. Environ. 39, 193–201. http://dx.doi.org/10.1016/j.atmosenv.2004.08.018.

Querol, X., Moreno, T., Karanasiou, A., Reche, C., Alastuey, A., Viana, M., Font, O., Gil, J., de Miguel, E., Capdevila, M., 2012. Variability of levels and composition of PM$_{10}$ and PM$_{2.5}$ in the Barcelona metro system. Atmos. Chem. Phys. 12, 5055–5076. http://dx.doi.org/10.5194/acp-12-5055-2012.

Salma, I., Weidinger, T., Maenhaut, W., 2007. Time-resolved mass concentration, composition and sources of aerosol particles in a metropolitan underground railway station. Atmos. Environ. 41, 8391–8405. http://dx.doi.org/10.1016/j.atmosenv.2007.06.017.

Sanders, P.G., Xu, N., Dalka, T.M., Maricq, M.M., 2003. Airborne brake wear debris: Size distributions, composition, and a comparison of dynamometer and vehicle tests. Environ. Sci. Technol. 37, 4060–4069. http://dx.doi.org/10.1021/es034145s.

Seaton, A., Cherrie, J., Dennekamp, M., Donaldson, K., Hurley, J.F., Tran, C.L., 2005. The London Underground: dust and hazards to health. Occup. Environ. Med. 62, 355–362. http://dx.doi.org/10.1136/oem.2004.014332.

Sundh, J., Olofsson, U., Olander, L., Jansson, A., 2009. Wear rate testing in relation to airborne particles generated in a wheel-rail contact. Lubr. Sci. 21, 135–150. http://dx.doi.org/10.1002/ls.80.